




István Ecsedi · Attila Baksa 

# Saint-Venant torsion of non-homogeneous orthotropic circular cylinder

Received: 5 July 2019 / Accepted: 7 November 2019 / Published online: 20 November 2019  
© The Author(s) 2019

**Abstract** The object of this paper is the Saint-Venant torsion of a radially non-homogeneous, hollow and solid circular cylinder made of orthotropic piezoelectric material. The elastic stiffness coefficients, piezoelectric constants and dielectric constants have only radial dependence. This paper gives the solution of the Saint-Venant torsion problem for torsion function, electric potential function, Prandtl's stress function and electric displacement potential function.

**Keywords** Piezoelectric · Saint-Venant torsion · Circular cylinder · Non-homogeneous

## 1 Introduction

Application of piezoelectric materials and structures has been increasing recently. Sensors and actuators are examples of active components made of piezoelectric materials which are used widely in smart structures. These structural components are often subjected to mechanical loading. The torsion of these structural members is an important task.

The Saint-Venant torsion of a homogeneous, isotropic elastic cylindrical body is a classical problem of elasticity [1–3], which is solved using a semi-inverse method by assuming a state of pure shear in the cylindrical body so that it gives rise to a resultant torque over the end cross sections. Extension of more complicated cases of anisotropic or non-homogeneous materials has been considered by Lekhnitskii [4,5], Rooney and Ferrari [6], Davi [7], Bisegna [8,9], Horgan and Chan [10], Rovenski et al. [11,12], Rovenski and Abramovich [13], Horgan [14], Ecsedi and Baksa [15,16].

In this paper, the torsional deformation of radially non-homogeneous, piezoelectric, solid and hollow circular cylinders is studied. This study gives a non-trivial generalization of the results in paper [8], which deals with the Saint-Venant torsion of radially non-homogeneous anisotropic elastic circular cylinder.

The formulation of the Saint-Venant's theory of uniform torsion for the homogeneous piezoelectric beams has been analyzed by Dave [7], Bisegna [8,9] and Rovenski et al. [11,12]. The papers of Bisegna [8,9] use the Prandtl's stress function and electric displacement potential function formulation for simply connected cross section. Davi [7] obtained a coupled boundary-value problem for the torsion function and for the electric potential function from a constrained three-dimensional static problem by the application of the usual assumptions of the Saint-Venant's theory. Rovenski et al. [11,12] give a torsion and electric potential function formulation of the Saint-Venant's torsional problem for monoclinic homogeneous piezoelectric beams. In these papers [11,12], a coupled Neumann problem is derived for the torsion and electric potential functions, where exact and numerical solutions for elliptical and rectangular cross sections are presented. Ecsedi and

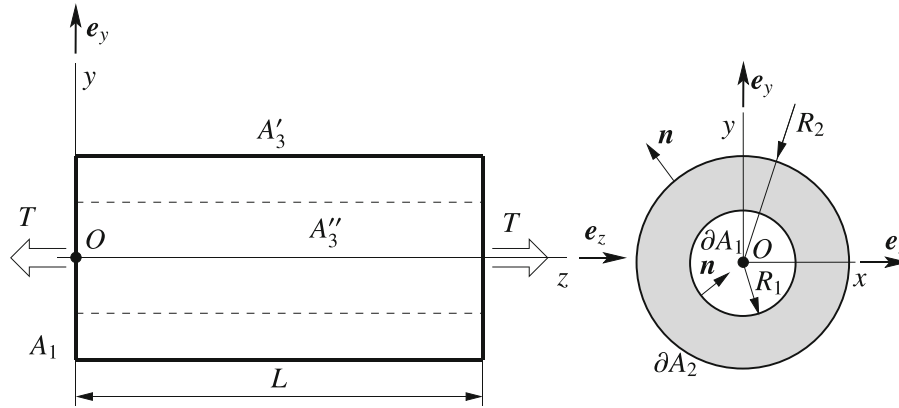


**Fig. 1** Hollow circular cylinder

Baksa [15] give a formulation of the Saint-Venant torsional problem for homogeneous monoclinic piezoelectric beams in terms of Prandtl's stress function and the electric displacement potential function. The Prandtl's stress function and electric displacement potential function satisfy a coupled Dirichlet problem in the multiply connected cross section. A direct formulation and a variational formulation are developed in [15]. In another paper by Ecsedi and Baksa [16], a variational formulation is presented for the torsional deformation of homogeneous linear piezoelectric monoclinic beams. The variational formulation presented uses the torsion and electric potential functions as independent quantities of the considered variational functional. The mechanical meaning of the variational functional defined in [16] is also given. Examples illustrate the application of the presented variational functional. Rovenski and Abramovich apply a linear analysis to piezoelectric beams with non-homogeneous cross sections that consist of various monoclinic (piezoelectric and elastic) materials [13]. They give the solution procedure for extension, bending, torsion and shear. The developed method is illustrated by numerical examples [13]. Batra et al. [17] studied the electromechanical nonlinear deformations of homogeneous, transversely isotropic piezoelectric circular cylinder loaded on its end cross sections. In [17], the second-order constitutive equations are used and show that when the cylinder is deformed by applying pure torque and non-electric charges at the end cross sections the potential difference between the end cross sections is proportional to the square of twist.

In this paper, the deformation of circular cylinders made of orthotropic, radially non-homogeneous piezoelectric material is studied by means of Saint-Venant's theory of uniform torsion. The elastic stiffness coefficients, piezoelectric constants and dielectric constants depend only on the radial coordinate. The dependence of material parameters is either described by smooth functions of radial coordinate as in the case of functionally graded materials [18, 19], or the material parameters are piecewise smooth functions of the radial coordinate as in the case of radially layered circular cylinders.

## 2 Formulation of Saint-Venant torsional problem

Let  $B = A \times (0, L)$  be a right circular cylinder of length  $L$ . Let  $A_1$  and  $A_2$  be the bases and  $A_3 = \partial A \times (0, L)$  the mantle of  $B$ . The cross section  $A$  is given in the Cartesian coordinate frame  $Oxyz$

$$A = \left\{ (x, y) \mid R_1^2 \leq x^2 + y^2 \leq R_2^2 \right\}. \quad (1)$$

The Cartesian coordinate frame  $Oxyz$  is supposed to be chosen in such a way that the  $Oz$ -axis is parallel to the generators of the cylindrical boundary surface segments  $A_3 = A_3' \cup A_3''$  (Fig. 1). The plane  $Oxy$  contains the terminal cross section  $A_1$ . The position of the end cross section  $A_2$  is given by  $z = L$ . A point  $P$  in  $B = B \cup A_1 \cup A_2 \cup A_3$  is indicated by the vector  $\mathbf{r} = x\mathbf{e}_x + y\mathbf{e}_y + z\mathbf{e}_z = \mathbf{R} + z\mathbf{e}_z$ , where  $\mathbf{e}_x$ ,  $\mathbf{e}_y$  and  $\mathbf{e}_z$  are the unit vectors of the coordinate system  $Oxyz$  (Figs. 1, 2).

In the case of Saint-Venant torsion, the displacement field  $\mathbf{u}$  and electric potential  $V$  of the twisted cylindrical bar can be represented as [11, 13]

$$\mathbf{u} = \vartheta z \mathbf{e}_z \times \mathbf{R} + \vartheta \omega(x, y) \mathbf{e}_z \quad (2)$$

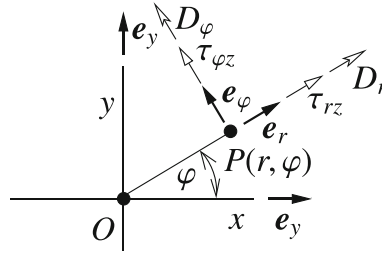


Fig. 2 Cylindrical coordinates  $(r, \varphi)$

$$V = \vartheta \phi(x, y), \quad (3)$$

where  $\vartheta$  is the rate of twist,  $\omega = \omega(x, y)$  is the torsion function and  $\phi = \phi(x, y)$  is the electric potential for the unit value of the twist. The vectorial product of the two vectors in Eq. 2 is denoted by cross. The shear strains are obtained from the linearized strain–displacement relationships of elasticity as [1,2]

$$\gamma_{xz} = \vartheta \left( \frac{\partial \omega}{\partial x} - y \right) \quad \gamma_{yz} = \vartheta \left( \frac{\partial \omega}{\partial y} + x \right). \quad (4)$$

The components of the electric field vectors are [11,12]

$$E_x = -\vartheta \frac{\partial \phi}{\partial x} \quad E_y = -\vartheta \frac{\partial \phi}{\partial y}. \quad (5)$$

The shearing stresses  $\tau_{xz}$ ,  $\tau_{yz}$  and electric displacements  $D_x$ ,  $D_y$  according to the constitutive equations of linear orthotropic piezoelectric bodies can be written in the next form:

$$\tau_{xz} = \tilde{A}_{55} \gamma_{xz} + \tilde{e}_{15} \frac{\partial V}{\partial x} = \vartheta \left[ \tilde{A}_{55} \left( \frac{\partial \omega}{\partial x} - y \right) + \tilde{e}_{15} \frac{\partial \phi}{\partial x} \right] \quad (6)$$

$$\tau_{yz} = \tilde{A}_{44} \gamma_{yz} + \tilde{e}_{24} \frac{\partial V}{\partial y} = \vartheta \left[ \tilde{A}_{44} \left( \frac{\partial \omega}{\partial y} + x \right) + \tilde{e}_{24} \frac{\partial \phi}{\partial y} \right] \quad (7)$$

$$D_x = \tilde{e}_{15} \gamma_{xz} - \tilde{\kappa}_{11} \frac{\partial V}{\partial x} = \vartheta \left[ \tilde{e}_{15} \left( \frac{\partial \omega}{\partial x} - y \right) - \tilde{\kappa}_{11} \frac{\partial \phi}{\partial x} \right] \quad (8)$$

$$D_y = \tilde{e}_{24} \gamma_{yz} - \tilde{\kappa}_{22} \frac{\partial V}{\partial y} = \vartheta \left[ \tilde{e}_{24} \left( \frac{\partial \omega}{\partial y} + x \right) - \tilde{\kappa}_{22} \frac{\partial \phi}{\partial y} \right]. \quad (9)$$

In Eqs. (6)–(9),  $\tilde{A}_{44}$  and  $\tilde{A}_{55}$  are the shear rigidities,  $\tilde{e}_{15}$  and  $\tilde{e}_{24}$  are the piezoelectric constants,  $\tilde{\kappa}_{11}$  and  $\tilde{\kappa}_{22}$  are the dielectric constants. In our case, the shear rigidities, the piezoelectric constants and the dielectric constants depend only on the radial coordinate

$$r = \sqrt{x^2 + y^2} \quad R_1 \leq r \leq R_2. \quad (10)$$

This dependence of the material parameters as a function of position is described by the inhomogeneity function  $f = f(r)$  as

$$\tilde{A}_{44} = f(r) A_{44} \quad \tilde{A}_{55} = f(r) A_{55} \quad (11)$$

$$\tilde{e}_{15} = f(r) e_{15} \quad \tilde{e}_{24} = f(r) e_{24} \quad (12)$$

$$\tilde{\kappa}_{11} = f(r) \kappa_{11} \quad \tilde{\kappa}_{22} = f(r) \kappa_{22}. \quad (13)$$

In Eqs. (11)–(13),  $A_{44}$ ,  $A_{55}$ ,  $e_{15}$ ,  $e_{24}$ ,  $\kappa_{11}$  and  $\kappa_{22}$  are constants and  $f = f(r)$  is unit free,  $f(r) > 0$ ,  $R_1 \leq r \leq R_2$ .

### 3 Solution of the torsion problem

Starting from the equation of mechanical equilibrium and Gauss equation, we can write

$$\frac{\partial \tau_{xz}}{\partial x} + \frac{\partial \tau_{yz}}{\partial y} = 0 \quad \frac{\partial D_x}{\partial x} + \frac{\partial D_y}{\partial y} = 0. \quad (14)$$

The substitution of Eqs. (6)–(9) into Eqs. (14)<sub>12</sub> gives the following results:

$$A_{55} \frac{\partial}{\partial x} \left[ f(r) \left( \frac{\partial \omega}{\partial x} - y \right) \right] + e_{15} \frac{\partial}{\partial x} \left[ f(r) \left( \frac{\partial \phi}{\partial x} \right) \right] + A_{44} \frac{\partial}{\partial y} \left[ f(r) \left( \frac{\partial \omega}{\partial y} + x \right) \right] + e_{24} \frac{\partial}{\partial y} \left( f(r) \frac{\partial \phi}{\partial y} \right) = 0 \quad (15)$$

$$e_{15} \frac{\partial}{\partial x} \left[ f(r) \left( \frac{\partial \omega}{\partial x} - y \right) \right] - \kappa_{11} \frac{\partial}{\partial x} \left( f(r) \frac{\partial \phi}{\partial x} \right) + e_{24} \frac{\partial}{\partial y} \left[ f(r) \left( \frac{\partial \omega}{\partial y} + x \right) \right] - \kappa_{22} \frac{\partial}{\partial y} \left( f(r) \frac{\partial \phi}{\partial y} \right) = 0. \quad (16)$$

The cylindrical surface  $A_3$  is stress free, i.e.,

$$\tau_{xz}n_x + \tau_{yz}n_y = 0 \quad \text{on } A_3. \quad (17)$$

There is no free charge on the cylindrical boundary surface, so we have

$$D_x n_x + D_y n_y = 0 \quad \text{on } A_3. \quad (18)$$

In Eqs. (17) and (18), the components of unit normal vector  $\mathbf{n}$  on the boundary curves  $\partial A_1 = \{(x, y) \mid x^2 + y^2 = R_1^2\}$  and  $\partial A_2 = \{(x, y) \mid x^2 + y^2 = R_2^2\}$  are (Fig. 1)

$$n_x = -\frac{x}{R_1} \quad n_y = -\frac{y}{R_1} \quad \text{on } \partial A_1 \quad (19)$$

$$n_x = \frac{x}{R_2} \quad n_y = \frac{y}{R_2} \quad \text{on } \partial A_2. \quad (20)$$

Detailed form of the stress boundary condition (17) and free charge boundary condition (18) are as follows:

$$A_{55}x \left( \frac{\partial \omega}{\partial x} - y \right) + e_{15}x \frac{\partial \phi}{\partial x} + A_{44}y \left( \frac{\partial \omega}{\partial y} + x \right) + e_{24}y \frac{\partial \phi}{\partial x} = 0 \quad (x, y) \in \partial A_1 \cup \partial A_2 \quad (21)$$

$$e_{15}x \left( \frac{\partial \omega}{\partial x} - y \right) - \kappa_{11}x \frac{\partial \phi}{\partial x} + e_{24}y \left( \frac{\partial \omega}{\partial y} + x \right) - \kappa_{22}y \frac{\partial \phi}{\partial y} = 0 \quad (x, y) \in \partial A_1 \cup \partial A_2. \quad (22)$$

Here, we note that, assuming sufficient smoothness of the inhomogeneity function  $f = f(\sqrt{x^2 + y^2})$ , the standard results from the linear theory of second-order partial differential equations show that the classical (strong) solutions to the boundary-value problem formulated by Eqs. (15–16) and Eqs. (21–22) are unique in two constants. This means that, if  $\omega = \omega(x, y)$  and  $\phi = \phi(x, y)$  are a solution, then

$$\tilde{\omega}(x, y) = \omega(x, y) + K_1 \quad \tilde{\phi}(x, y) = \phi(x, y) + K_2 \quad (23)$$

are also a solution with arbitrary values of constants  $K_1$  and  $K_2$ .

**Theorem 1** *The solution of the torsional boundary-value problem formulated by Eqs. (15–16) and Eqs. (21–22) is*

$$\omega(x, y) = C_\omega xy + K_1 \quad (24)$$

$$\phi(x, y) = C_\phi xy + K_2, \quad (25)$$

where

$$C_\omega = \frac{(A_{55} - A_{44})(\kappa_{11} + \kappa_{22}) + e_{15}^2 + e_{24}^2}{(A_{55} + A_{44})(\kappa_{11} + \kappa_{22}) + (e_{15} + e_{24})^2} \quad (26)$$

$$C_\phi = -\frac{2(A_{44}e_{15} - A_{55}e_{24})}{(A_{55} + A_{44})(\kappa_{11} + \kappa_{22}) + (e_{15} + e_{24})^2} \quad (27)$$

$K_1$  and  $K_2$  are arbitrary real constants.

*Proof* By the direct substitution of the following equations:

$$\begin{aligned} \frac{\partial \tilde{A}_{ij}}{\partial x} &= f'(r) \frac{x}{r} A_{ij} & \frac{\partial A_{ij}}{\partial y} &= f'(r) \frac{y}{r} A_{ij} \\ i, j &= 4, 5, & i &\neq j \end{aligned} \quad (28)$$

$$\begin{aligned} \frac{\partial \tilde{e}_{mn}}{\partial x} &= f'(r) \frac{x}{r} e_{mn} & \frac{\partial \tilde{e}_{mn}}{\partial y} &= f'(r) \frac{y}{r} e_{mn} \\ m &= 1, 2 & n &= 4, 5 \end{aligned} \quad (29)$$

$$\frac{\tilde{\kappa}_{pp}}{\partial x} = f'(r) \frac{x}{r} \kappa_{pp} \quad \frac{\tilde{\kappa}_{pp}}{\partial y} = f'(r) \frac{y}{r} \kappa_{pp} \quad p = 1, 2, \quad (30)$$

we get the functions  $\omega = \omega(x, y)$  and  $\phi = \phi(x, y)$  given by Eqs. (20) and (27) with arbitrary constants  $K_1$  and  $K_2$  satisfying Eqs. (15–16) and Eqs. (21–22). Next, we define  $K_1 = 0$  and  $K_2 = 0$  according to the statement formulated by Eq. (23).  $\square$

#### 4 Shearing stresses and electric displacement field

Shearing stresses are obtained from Eqs. (6) and (7):

$$\tau_{xz} = \vartheta f(r) [A_{55}(C_\omega - 1) + e_{15}C_\phi] y \quad (31)$$

$$\tau_{yz} = \vartheta f(r) [A_{44}(C_\omega + 1) + e_{24}C_\phi] x. \quad (32)$$

In the cylindrical coordinate system,

$$r = \sqrt{x^2 + y^2} \quad \varphi = \arctan \frac{y}{x} \quad (33)$$

$$x = r \cos \varphi \quad y = r \sin \varphi \quad (34)$$

$$\begin{aligned} \tau_{rz} &= \tau_{xz} \cos \varphi + \tau_{yz} \sin \varphi \\ &= \vartheta f(r) [A_{55}(C_\omega - 1) + e_{15}C_\phi] r \cos \varphi \sin \varphi + \vartheta f(r) [A_{44}(C_\omega + 1) + e_{24}C_\phi] r \cos \varphi \sin \varphi = 0 \end{aligned} \quad (35)$$

$$\begin{aligned} \tau_{\varphi z} &= -\tau_{xz} \sin \varphi + \tau_{yz} \cos \varphi = -\vartheta f(r) [A_{55}(C_\omega - 1) + e_{15}C_\phi] r \sin^2 \varphi + \vartheta f(r) [A_{44}(C_\omega + 1) + e_{24}C_\phi] r \cos^2 \varphi \\ &= 2\vartheta f(r) \frac{A_{55}A_{44}(\kappa_{11} + \kappa_{22}) + A_{55}e_{24}^2 + A_{44}e_{15}^2}{(A_{55} + A_{44})(\kappa_{11} + \kappa_{22}) + (e_{15} + e_{24})^2} r. \end{aligned} \quad (36)$$

The computation of the components of the electric displacement vector is based on Eqs. (8–9):

$$D_x = \vartheta f(r) [e_{15}(C_\omega - 1)y - \kappa_{11}C_\phi y] \quad (37)$$

$$D_y = \vartheta f(r) [e_{24}(C_\omega + 1)x - \kappa_{22}C_\phi x]. \quad (38)$$

In the cylindrical coordinate system, the components of the electric displacement vectors are  $D_r$  and  $D_\varphi$ , which are computed as

$$D_r = D_x \cos \varphi + D_y \sin \varphi = \vartheta f(r) [e_{15}(C_\omega - 1) - \kappa_{11}C_\phi + e_{24}(C_\omega + 1) - \kappa_{22}C_\phi] r \cos \varphi \sin \varphi = 0 \quad (39)$$

$$\begin{aligned} D_\varphi &= -D_x \sin \varphi + D_y \cos \varphi = -\vartheta f(r) [e_{15}(C_\omega - 1) - \kappa_{11}C_\phi] r \sin^2 \varphi + \vartheta f(r) [e_{24}(C_\omega + 1) - \kappa_{22}C_\phi] r \cos^2 \varphi \\ &= 2\vartheta f(r) \frac{e_{15}A_{44}\kappa_{22} + e_{24}A_{55}\kappa_{11} + e_{15}e_{24}(e_{15} + e_{24})}{(A_{55} + A_{44})(\kappa_{11} + \kappa_{22}) + (e_{15} + e_{24})^2} r. \end{aligned} \quad (40)$$

The connection between the applied torque  $T$  and the rate of twist  $\vartheta$  is characterized by mechanical torsional rigidity  $S_M$  which is defined as

$$S_M = \frac{T}{\vartheta}, \quad (41)$$

where

$$T = 2\pi \int_{R_1}^{R_2} r^2 \tau_{\varphi z}(r) dr. \quad (42)$$

The combination of Eq. (36) with Eqs. (41) and (42) gives

$$S_M = 4\pi F \frac{A_{55}A_{44}(\kappa_{11} + \kappa_{22}) + A_{44}e_{15}^2 + A_{55}e_{24}^2}{(A_{44} + A_{55})(\kappa_{11} + \kappa_{22}) + (e_{15} + e_{24})^2}, \quad (43)$$

where

$$F = \int_{R_1}^{R_2} r^3 f(r) dr. \quad (44)$$

Based on Eqs. (36) and (43), a simple computation gives the next result for the shearing stress in terms of the applied torque:

$$\tau_{\varphi z} = \frac{T}{2\pi F} r f(r). \quad (45)$$

Electrical torsional rigidity  $S_E$  is defined as

$$S_E = \frac{1}{\vartheta} \int_A r D_\varphi dA. \quad (46)$$

Starting from Eq. (40), after a simple computation we get

$$S_E = 4\pi F \frac{(e_{15} + e_{24})e_{15}e_{24} + e_{15}A_{44}\kappa_{22} + e_{24}A_{55}\kappa_{11}}{(A_{44} + A_{55})(\kappa_{11} + \kappa_{22}) + (e_{15} + e_{24})^2}. \quad (47)$$

It is very easy to prove that, in terms of the applied torque  $T$ , the circumferential component of the electric displacement vector can be computed from the following equation:

$$D_\varphi = T \frac{S_E}{S_M} \frac{f(r)}{2\pi F} r. \quad (48)$$

The solution of the Saint-Venant torsion problem of orthotropic FGM circular cylinder in the case of radial dependence of material parameters has two important properties:

- The torsion function  $\omega = \omega(x, y)$  and the electric potential function  $\phi = \phi(x, y)$  are independent of the inhomogeneity of the cross section.
- For a given torque  $T$ , the stress field is independent of the material parameters ( $A_{44}$ ,  $A_{55}$ ,  $e_{15}$ ,  $e_{24}$ ,  $\kappa_{11}$  and  $\kappa_{22}$ ) and it depends only on the non-homogeneity of the considered circular cross section.

Here, we note that, in the case of anisotropic non-homogeneous linearly elastic circular cylinder, the torsion function is also independent of the radial inhomogeneity [20].

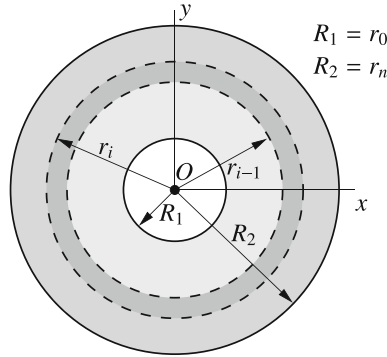


**Fig. 3** Layered hollow circular cross section

### 5 Prandtl's stress function, electric displacement potential function

The determination of the Prandtl's stress function  $U = U(r, \varphi)$  is based on the following equations:

$$\tau_{rz} = \vartheta \frac{1}{r} \frac{\partial U}{\partial \varphi} = 0 \quad (49)$$

$$\tau_{\varphi z} = -\vartheta \frac{\partial U}{\partial r} = 2\vartheta f(r)r \frac{A_{55}A_{44}(\kappa_{11} + \kappa_{22}) + A_{55}e_{24}^2 + A_{44}e_{15}^2}{(A_{44} + A_{55})(\kappa_{11} + \kappa_{22}) + (e_{15} + e_{24})^2}. \quad (50)$$

Equation (49) shows that  $U$  does not depend on the polar angle  $\varphi$ . In the next part of this paper, we consider only a simply connected (solid) cross section, that is  $R_1 = 0$ ,  $R_2 = R$ . It is known that the Prandtl's stress function satisfies the homogeneous boundary condition:

$$U(R) = 0. \quad (51)$$

The integration of Eq. (50) under the boundary condition (51) gives

$$U(r) = 2 \frac{A_{55}A_{44}(\kappa_{11} + \kappa_{22}) + A_{55}e_{24}^2 + A_{44}e_{15}^2}{(A_{55} + A_{44})(\kappa_{11} + \kappa_{22}) + (e_{15} + e_{24})^2} \int_r^R \rho f(\rho) d\rho. \quad (52)$$

By the same method, we can obtain the electric displacement potential function as is used in the derivation of Eq. (52). We note that, for solid cross section, the electric displacement potential function  $H = H(r)$  satisfies the boundary condition [9, 15]:

$$H(R) = 0. \quad (53)$$

A detailed computation, starting from the equations

$$D_r = \vartheta \frac{1}{r} \frac{\partial H}{\partial \varphi} = 0 \quad (54)$$

$$D_\varphi = -\vartheta \frac{\partial H}{\partial r} = 2\vartheta f(r)r \frac{e_{15}A_{44}\kappa_{22} + e_{24}A_{55}\kappa_{11} + e_{15}e_{24}(e_{15} + e_{24})}{(A_{55} + A_{44})(\kappa_{11} + \kappa_{22}) + (e_{15} + e_{24})^2}, \quad (55)$$

gives

$$H(r) = 2 \frac{e_{15}A_{44}\kappa_{22} + e_{24}A_{55}\kappa_{11} + e_{15}e_{24}(e_{15} + e_{24})}{(A_{55} + A_{44})(\kappa_{11} + \kappa_{22}) + (e_{15} + e_{24})^2} \int_r^R \rho f(\rho) d\rho. \quad (56)$$

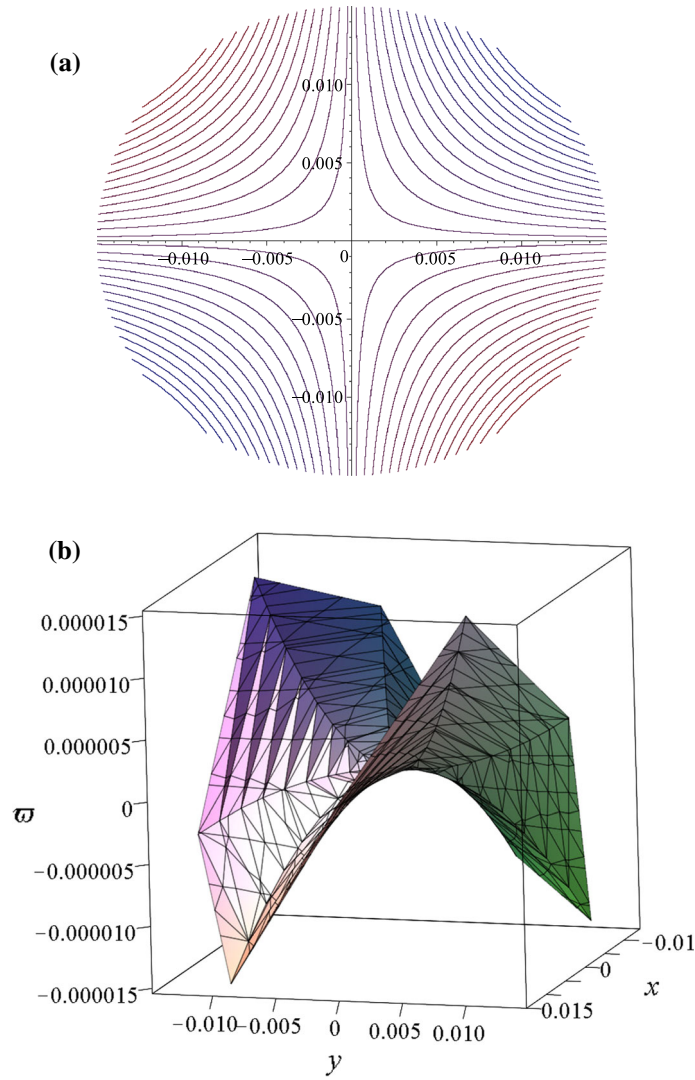


**Fig. 4** Illustrations of the torsion function: **a** contour lines, **b** graph of the torsion function

**6 Layered non-homogeneous circular cross section**

Figure 3 shows a hollow circular cross section which is layered in the radial direction. In this case, the inhomogeneity function is piecewise continuous on the cross-sectional domain and it is given by the following formula:

$$f(r) = f_i(r) \quad r_{i-1} < r < r_i$$

$$(i = 1, 2, \dots, n) \quad r_0 = R_1 \quad r_n = R_2 \tag{57}$$

It is evident for radially layered, non-homogenous, orthotropic piezoelectric hollow circular cross section that the torsion function and the electric potential function given by Eqs. (24), (25), together with all the formulae obtained before, are valid here, and we have

$$\int_{R_1}^{R_2} \rho^3 f(\rho) d\rho = \sum_{i=1}^n \int_{r_{i-1}}^{r_i} \rho^3 f_i(\rho) d\rho. \tag{58}$$



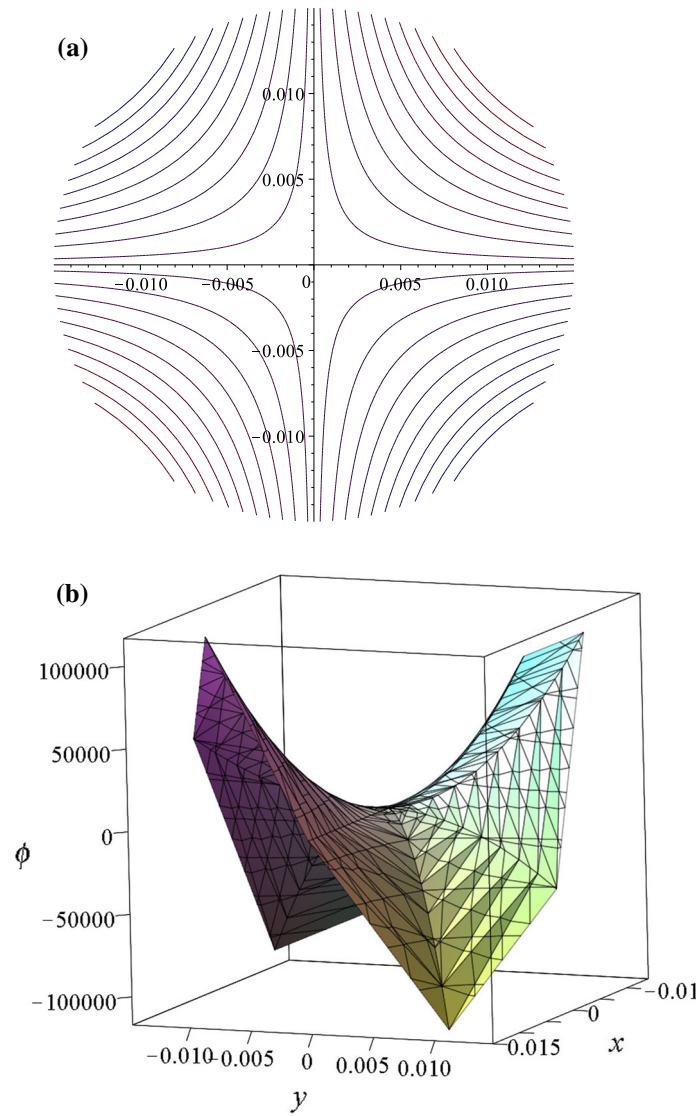


Fig. 5 Plots of electric potential function: **a** contour lines, **b** graph of the electric potential function

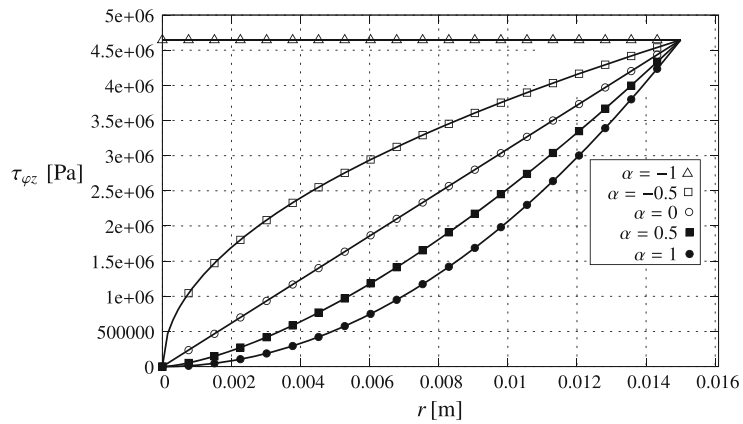


Fig. 6 Plots of shearing stress

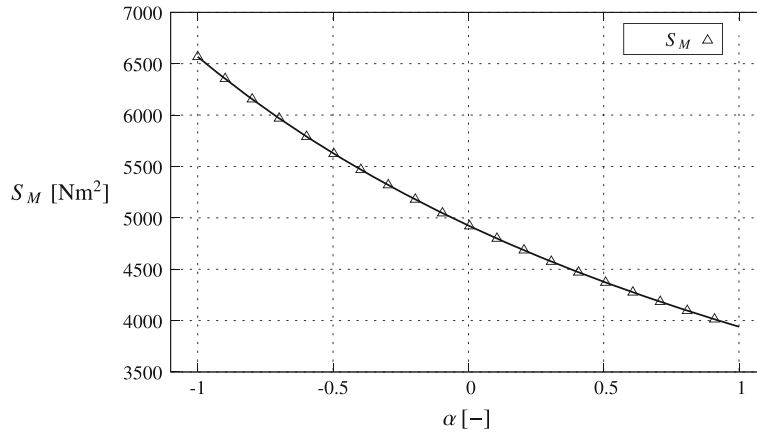


Fig. 7 Dependence of mechanical torsional rigidity from  $\alpha$

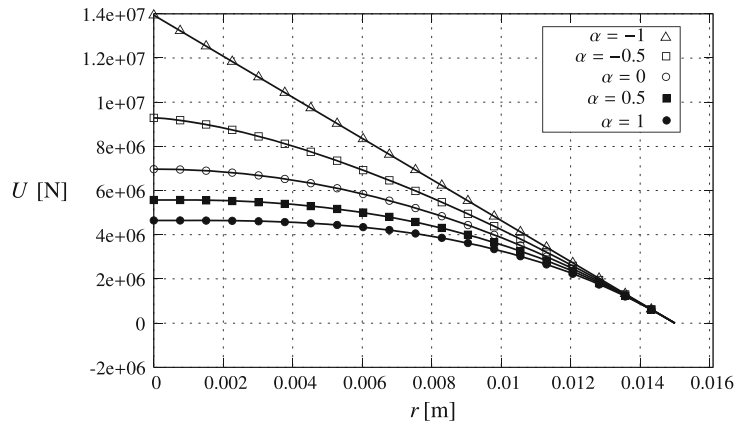


Fig. 8 Dependence of Prandtl's stress function from  $\alpha$

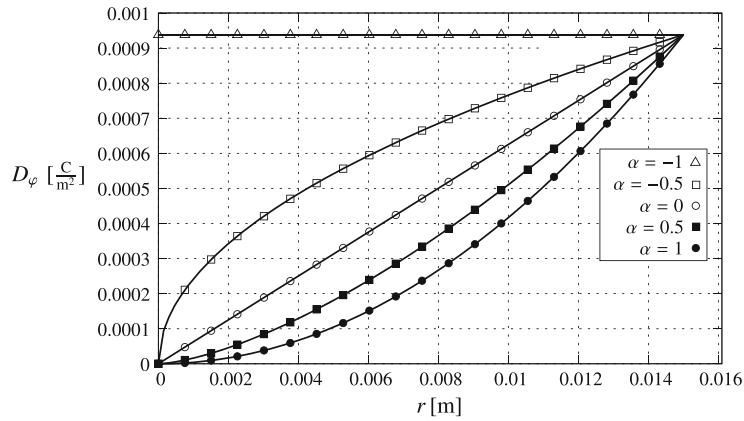


Fig. 9 Plots of  $D_\varphi$

The continuity conditions of torsional function and electric potential function over the whole cross section are satisfied. This fact follows from Eqs. (24) and (25). The continuity conditions of shearing stress  $\tau_{rz}$  and electric displacement  $D_r$  are also fulfilled, since on the whole cross section  $\tau_{rz}$  and  $D_r$  vanish.

Here, we note that, from the obtained results, we can recover the solution of the Saint-Venant torsion for radially non-homogeneous orthotropic elastic circular cylinder. This fact is illustrated in the cases of torsion function and torsional rigidity. For orthotropic elastic material, we have

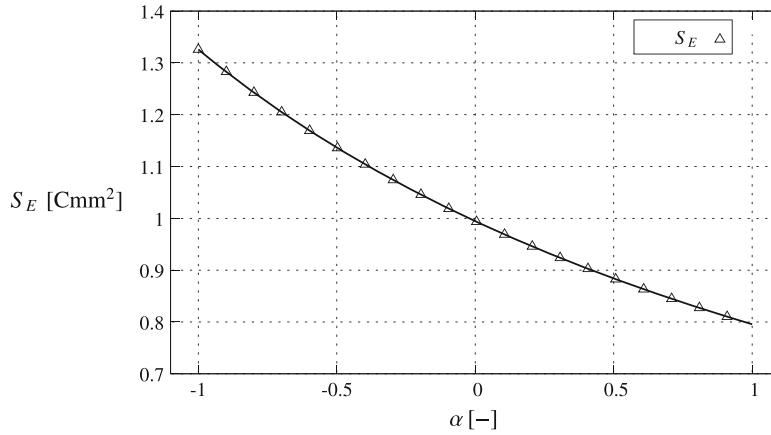


Fig. 10 Dependence of electrical torsional rigidity from  $\alpha$

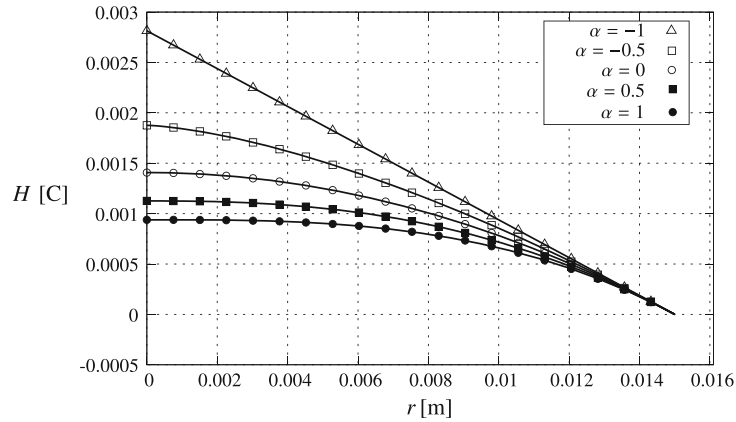


Fig. 11 Dependence of electric displacement potential function from  $\alpha$

$$e_{15} = e_{24} = 0. \tag{59}$$

From Eqs. (24), (26) and (59), it follows that for radially inhomogeneous Cartesian orthotropic elastic beams

$$\omega(x, y) = \frac{A_{55} - A_{44}}{A_{55} + A_{44}} xy. \tag{60}$$

Furthermore, in this case the following result can be derived for the torsional rigidity from (43):

$$S = 4\pi F \frac{A_{55}A_{44}}{A_{44} + A_{55}}. \tag{61}$$

### 7 Example

The following data are used in the numerical example:

$$\begin{aligned} A_{44} &= 6.27 \times 10^{10} \text{ Pa}; & A_{55} &= 5.13 \times 10^{10} \text{ Pa} \\ e_{15} &= 17 \text{ C/m}^2; & e_{24} &= 9 \text{ C/m}^2 \\ \kappa_{11} &= 2.0797 \times 10^{-9} \text{ F/m}; & \kappa_{22} &= 2.186 \times 10^{-9} \text{ F/m} \\ R_1 &= 0; & R_2 = R &= 0.015 \text{ m} \\ \vartheta &= 0.5 \times 10^{-2} \text{ rad/m}; & f(r, \alpha) &= \left(\frac{r}{R}\right)^\alpha. \end{aligned}$$

The contour lines and the graph of the torsion function  $\omega$  are shown in Fig. 4 for  $\alpha = 1$ . In Fig. 5, the contour lines and the graph of the electric potential function  $\phi$  are presented for  $\alpha = 1$ . For  $\alpha = -1, \alpha = -0.5, \alpha = 0, \alpha = 0.5$  and  $\alpha = 1$ , the graphs of shearing stress  $\tau_{\varphi z}$  are shown in Fig. 6. The dependence of mechanical torsional rigidity  $S_M$  from the graded index  $\alpha$  is shown in Fig. 7.

The dependence of Prandtl's stress function  $U$  from the graded index  $\alpha$  is shown in Fig. 8. For  $\alpha = -1, \alpha = -0.5, \alpha = 0, \alpha = 0.5$  and  $\alpha = 1$ , the graphs of electric displacement  $D_\varphi$  are shown in Fig. 9. The electric torsional rigidity as a function of  $\alpha$  is shown in Fig. 10. The dependence of electric displacement potential function  $H$  from  $\alpha$  is illustrated in Fig. 11.

## 8 Conclusions

The purpose of this paper is to investigate the effects of the radial inhomogeneity of the material to the torsional response of a linearly piezoelectric, orthotropic circular cylinder. The elastic stiffness coefficients, piezoelectric constants and dielectric constants have radial dependence. It is shown that the considered problem of Saint-Venant torsion has two important properties:

- The torsion function and the electric potential function are independent of the cross-sectional inhomogeneity.
- For the given torque, the stress field is independent of the material parameters; it depends only on the non-homogeneity of the cross section.

The presented exact analytical solution can be used as a benchmark solution to verify the efficiency of the usual approximate methods, such as finite element and finite difference methods.

**Acknowledgements** Open access funding provided by University of Miskolc (ME). The described article/presentation/study was carried out as part of the EFOP-3.6.1-16-00011 “Younger and Renewing University—Innovative Knowledge City—institutional development of the University of Miskolc aiming at intelligent specialization” project implemented in the framework of the Szechenyi 2020 program. The realization of this project is supported by the European Union, co-financed by the European Social Fund. This research was (partial) carried out in the framework of Center of Excellence of Innovative Engineering Design and Technologies at the University of Miskolc and supported by the National Research Development and Innovation Office—NKFIH K115701.

**Open Access** This article is distributed under the terms of the Creative Commons Attribution 4.0 International License (<http://creativecommons.org/licenses/by/4.0/>), which permits unrestricted use, distribution, and reproduction in any medium, provided you give appropriate credit to the original author(s) and the source, provide a link to the Creative Commons license, and indicate if changes were made.

## Compliance with ethical standards

**Conflict of interest** The authors declare that they have no conflict of interest.

## References

1. Lurie, A.I.: Theory of Elasticity. Fiz-Mat-Lit., Moscow (1970). (In Russian)
2. Sokolnikoff, I.S.: Mathematical Theory of Elasticity. McGraw Hill, New York (1956)
3. Sadd, M.: Theory, Applications and Numerics. Elsevier, Amsterdam (2005)
4. Lekhnitskii, S.G.: Torsion of Anisotropic and Non-homogeneous Beams. Nauka, Moscow (1971). (In Russian)
5. Lekhnitskii, S.G.: Theory of Elasticity of an Anisotropic Body. Mir. Publishers, Moscow (1981). (In Russian)
6. Rooney, F.T., Ferrari, M.: Torsion and flexure of inhomogeneous elements. Compos. Eng. **5**(7), 901–911 (1995)
7. Davi, F.: Saint-Venant's problem for linear piezoelectric bodies. J. Elast. **43**, 227–245 (1996)
8. Bisegna, P.: The Saint-Venant problem in the linear problem of piezoelectricity. Atti Convegno Lincei. Accad. Naz. Lincei Rome **40**, 151–165 (1998)
9. Bisegna, P.: The Saint-Venant problem for monoclinic piezoelectric cylinders. ZAMM **78**(3), 147–165 (1999)
10. Horgan, C.O., Chan, A.M.: Torsion of functionally graded isotropic linearly elastic bars. J. Elast. **52**(2), 181–189 (1999)
11. Rovenski, V., Harash, E., Abramovich, H.: Saint-Venant's problem for homogeneous piezoelectric beams. TAE Report No. 967, 1–100 (2006)
12. Rovenski, V., Harash, E., Abramovich, H.: Saint-Venant's problem for homogeneous piezoelectric beams. J. Appl. Mech. **47**(6), 1095–1103 (2007)
13. Rovenski, V., Abramovich, H.: Saint-Venant problem for computed piezoelectric beams. J. Elast. **96**, 105–127 (2009)
14. Horgan, C.O.: On the torsion of functionally graded anisotropic linearly elastic bars. IMA J. Appl. Math. **72**(5), 556–562 (2007)

15. Ecsedi, I., Baksa, A.: Prandtl's formulation for the Saint-Venant's torsion of homogeneous piezoelectric beams. *Int. J. Solids Struct.* **47**, 3076–3083 (2010)
16. Ecsedi, I., Baksa, A.: A variational formulation for the torsion problem of piezoelectric beams. *Appl. Math. Model.* **36**, 1668–1677 (2012)
17. Batra, R.C., Dell'Isola, F., Vidoli, S.: A second order solution of Saint-Venant's problem for a piezoelectric circular bar using Signorini's perturbation method. *J. Elast.* **52**(1), 75–90 (1998)
18. Shen, H.S.: *Functionally Graded Materials. Nonlinear Analysis of Plates and Shells.* CRC Press, New York (2009)
19. Suresh, S.M.: *Fundamentals of Functionally Graded Materials.* IOM Communications Limited, London (1998)
20. Ecsedi, I., Baksa, A.: Torsion of functionally graded anisotropic linearly elastic circular cylinder. *Eng. Trans.* **66**(4), 413–426 (2018)

**Publisher's Note** Springer Nature remains neutral with regard to jurisdictional claims in published maps and institutional affiliations.